BACHELOR

Characteristics of hydrogen peroxide production using a dielectric barrier discharge

van de Ven, T.H.M.

Award date:
2011

Characteristics of hydrogen peroxide production using a dielectric barrier discharge

T.H.M. van de Ven EPG 11-13

Date:
November 2011
Student ID:
0640484
Supervisors:
Christopher A. Vasko, Peter J. Bruggeman

Elementary Processes in Gas Discharges (EPG)
University of Technology Eindhoven

Abstract

The characteristics of a H_2O_2 producing dielectric barrier discharge (DBD) at atmospheric pressure and room temperature is studied. The DBD operates at 30 to 60 kHz AC voltages and at powers up to 2 W. The volume of the plasma is small (0.35 cm^3). Humid helium and a mixture of helium with 2% H_2 and 2% O_2 are used. The focus of this study is on the efficiency of the process.

H_2O_2 production is measured in the liquid phase using a spectrophotometric method which uses the reaction of H_2O_2 with ammonium metavanadate. Powers are calculated using Lissajous figures from the voltage $V(t)$ plotted versus the charge $C(t)$ in the DBD. The gas temperature was firstly obtained by acquiring the rotational temperature of N_2 by fitting the N_2(C-B)(0-0) rotational band and secondly by obtaining a Boltzmann plot of resolved rotational OH(A-X) lines. A temperature of 350 $\pm$ 50 K is found. Any fluctuations of the temperature remained within the experimental accuracy therefore no temperature dependency of the efficiency is determined.

Using humid helium it is shown that the production increases with power and water content. The efficiency shows a peak around 1 watt and saturation at higher powers. Agains expectations using pulsed power decreases the production and efficiency.

Using the H_2O_2 mixture it is shown that the production is not dependent on the power. With a pulsed power applied the production increases, in contrary to the humid helium.

The results indicate that a minimum residence time is needed for an efficient H_2O_2 production. Comparison with literature confirms this result.

This work is part of a 10 weeks long internship for the concluding project of the bachelor Applied Physics. The research is done in the framework of a STW project and a PhD thesis on the production of hydrogen peroxide.

Contents

Chapter 1

Introduction

Hydrogen peroxide (H_2O_2) is a widely used versatile chemical that is produced on large scales by the anthraquinone process. Because this process is complex and therefore expensive, numerous new production techniques are investigated [9]. Recently the production of H_2O_2 by direct synthesis from humid carrier gases or O_2-H_2 mixtures with atmospheric plasmas is examined. This process has proved to be efficient for larger volume reactors [22] but in this work the possibilities to use micro plasma reactors is investigated.The used gases are humid helium and a mixture of helium with hydrogen and oxygen. An AC driven dielectric barrier discharge (DBD) operating at atmospheric pressure and room temperature will be used. For this DBD and the setup as a whole, the characteristics will be investigated. The focus will be on the H_2O_2 production efficiency.

According to literature high efficiencies up to 80,8 g kWh^{-1} can be reached [22]. However, the used DBDs usualy differ in properties as size, used flow rates [22], different gas mixtures [5] [11] [12] or they have some sort of cooling mechanism [23]. A comparable DBD was used by Kirkpatrick *et al.* who obtained efficiencies and production rates of 0.14 g kWh^{-1} [12]. A selection of efficiencies along with the used powers from literature is presented in table 1.1

Gas mixture	Type of discharge	Power (W)	Efficiency (g kWh^{-1})
Humid gas	Atmospheric DBD using Ar, liquid film	1,50	1,7
Humid gas	Atmospheric DBD using Ar	1,33	0.14
Humid gas	Pulsed DBD with steam	40,0	0.40
H_2 + O_2 mixture	Microwave with cold trap		0.61
H_2 + O_2 mixture	Dielectric barrier discharge	11.,9	12.50
H_2 + O_2 mixture	Dielectric barrier discharge	3.50	80.00

Table 1.1: Efficiencies reported in various literatures from Locke *et al.* [16].

With the used setup the following parameters can be varied: the power and the duty cycle provided by the power source, the amount of flow and the composition of the gas mixture. In this work the influence of all these parameter is investigated.

After a short introduction on the DBD the experimental setup is described. Hereafter the results of the experiments are presented and discussed.

1.1 Dielectric barrier discharges

The DBD produces a relatively cold, non-equilibrium plasma at atmospheric pressure. First reported experiments on DBDs where made over a century ago by Siemens in 1857. Since then they where mainly developed for the production of ozone, where a flow of oxygen was exposed to a plasma generated between the electrodes of the DBD. The novelty about this device was that the electrodes are placed outside the discharge. A dielectric barrier is used to separate one or both electrodes from the plasma.

Because of the ozone producing capabilities the DBD was subject to extensive researches. Besides more efficient ozone production this also resulted in numerous other applications: surface modification, plasma chemical vapor deposition, pollution control, excitation of CO_2 lasers and excimer lamps and large-area flat plasma display panels.

Because of the dielectric barrier the DBD needs an alternating current to operate. To transport current in the discharge the electric field has to be high enough to cause breakdown in the gas. Therefore voltages in the range of a few hundred volt to several kilovolts are required.

In most gases, the breakdown happens in a large number of micro discharges. The plasma is therefore normally filamentary, but in helium and helium-rich mixtures, as the ones used in this work, diffuse discharges can be obtained. Each individual micro discharge can be regarded as a miniature plasma chemical reactor. Scaling up or increasing the power density just means that more micro discharges are initiated per unit of time and per unit of electrode area [13].

The gas in between the micro discharges serves as a reservoir which absorbs the energy dissipated by the discharges. This way the filamentary nature ensures a quick heat removal. This is reinforced by high thermal conductivity of the used helium. Also the relatively high operating pressure results in a high collision rate between electrons and other particles, which stimulates heat exchange. However, the fast heat removal and the current limited by the dielectric barrier cause the gas temperature to be much lower than the electron temperature.

The early phases of micro discharge formation are characterized by electron multiplication, by excitation and dissociation processes initiated by energetic electrons, and by ionization processes and space charge accumulation. The ionic and excited atomic and molecular species initiate chemical reactions that finally result in the synthesis of a desired species like ozone or H_2O_2. Most reactions involve neutral species, like atoms, and therefore fall under the free-radical chemistry. The next section will deal with the chemistry of the plasmas used in this work.

1.2 Plasma reactions

The most important reaction for the production of H_2O_2 is the one where two OH radicals react to a H_2O_2 molecule:

$$OH + OH \longrightarrow H_2O_2$$

Therefore the production and consumption of the OH radical is of even importance. Reactions involving OH are numerous. Some of them produce OH, which is beneficial for the production of H_2O_2, but others consume OH. Liu *et al.* used simulations to determine the most important reactions at room temperature [15]. The most important reactions in helium and water mixtures are listed in table 1.2.

Reaction	Rate k (cm^3s^{-1})	
Production reaction		
$OH + OH + M \rightarrow H_2O_2 + M$	$3.84 \times 10^{-12} \exp(373/T)$	[1]
Promoting reactions		
$e^- + H_2O^+ \rightarrow OH + H$	2.6×10^{-14}	[2]
$H^- + H_2O^+ \rightarrow OH + H_2$	$2.25 \times 10^{-10} \exp(-10515/T)$	[8]
$He_2^+ + H_2O \rightarrow OH + HeH^+ + He$ [(a)]	2.10×10^{-10}	[8]
$O + H_2 \rightarrow OH + H$ [(b)]	$5.51 \times 10^{-11} \exp(5000/T)$	[1]
$O_2 + H \rightarrow OH + H$ [(b)]	$3.08 \times 10^{-10} \exp(-8130/T)$	[1]
$e^- + H_2 \rightarrow 2H + e^-$ [(b)]	$8.73 \times 10^{-8} T_e^{-0.5} \exp(11.7/T_e)$	[8]
$e^- + O_2 \rightarrow 2O + e^-$ [(b)]	$6.86 \times 10^{-9} \exp(-6.29/T_e)$	[1]
$e^- + O_2 \rightarrow O + O^-$ [(b)]	$1.07 \times 10^{-9} T_e^{-1.391} \exp(-66/T_e)$	[1]
Dissociative reactions		
$H_2O_2 \rightarrow 2\ OH$	$3.35 \times 10^{-7} \exp(-23093/T)$	[1]
$H + H_2O_2 \rightarrow H_2O + OH$ [(b)]	$4.0 \times 10^{-11} \exp(-2000/T)$	[10]
$e^- + H_2O_2 \rightarrow 2OH + e^-$	2.36×10^{-9}	[19]
$e^- + H_2O_2 \rightarrow H + HO_2 + e^-$	3.1×10^{-11}	[19]
$e^- + H_2O_2 \rightarrow H_2O + O^-$	$1.57 \times 10^{-10} T_e^{-0.55}$	[19]
$e^- + H_2O_2 \rightarrow OH + OH^-$	$2.7 \times 10^{-10} T_e^{-0.5}$	[19]
Demoting reactions		
$OH + OH \rightarrow H_2O + O$	$4.2 \times 10^{-12} \exp(-240/T)$	[10]
$OH + H + M \rightarrow H_2O + M$ [(b)]	$2.57 \times 10^{-10} \exp(-84/T)$	[1]
$OH + HO_2 \rightarrow H_2O + O_2$	$4.8 \times 10^{-11} \exp(250/T)$	[10]
$OH + H_2O \rightarrow HO_2 + H_2O$	$2.9 \times 10^{-12} \exp(-160/T)$	[10]

Table 1.2: Reaction rates of important reactions from literature. T is the gas temperature in K, T_e is the electron temperature in eV.
[(a)] *Only for small concentrations of water.*
[(b)] *Especially important when using the H_2 -O_2 mixture.*

As can be seen from the table some reaction rates are gas or electron temperature dependent. This implies that the H_2O_2 production, which involves all of the above mentioned reactions, is also dependent of both temperatures. The reactions influenced most by temperature are plotted in figure 1.1.

The reaction rate of the creation of H_2O_2 from two OH radicals decreases rapidly with the gas temperature while OH dissipating reactions increase. This

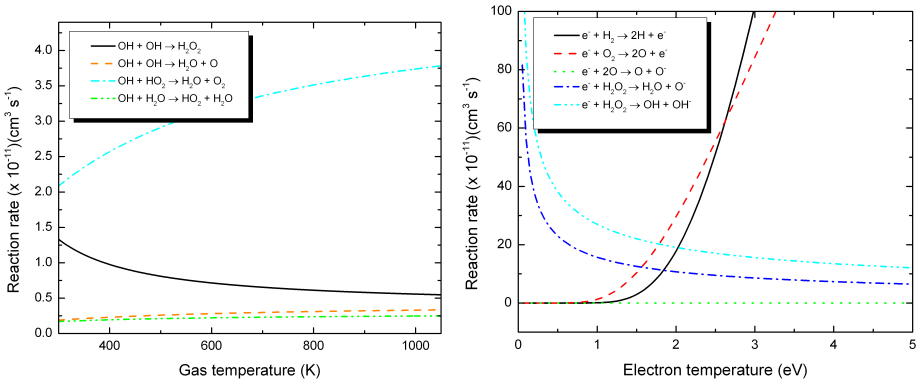

(a) Gas temperature. (b) Electron temperature

Figure 1.1: The reaction rates of important reactions plotted versus temperature.

implies that the production of H_2O_2 will be decrease with the gas temperature.

There are two options that can be used to improve the efficiency of the H_2O_2 production: using a stoichiometric mixture or a pulsed power source.

In this work a stoichiometric mixture of hydrogen and oxygen is used. The stoichiometry should improve the selectivity of the reactions in the plasma. As can be seen from table 3.1 high efficiencies can be reached with such mixtures.

When a pulsed power source used it is expected that gas temperatures decreases since the gas has time to cool between pulses. The overall power applied in the pulsed mode is the same as in the case of a continuous power signal, but therefore the voltages applied and the power during the pulses will higher. The electron temperature is therefore expected to be higher during the pulsed mode. From figure 1.1b it can be seen that the dissociation rate of H_2O_2 is lower for higher electron temperatures. On the other hand, the radical density of H and O will increase strongly with electron temperature, which can be used in H_2O_2 forming reactions. The efficiency is therefore expected to increase when the pulsed mode is used.

Chapter 2

Experimental

2.1 Setup

The parallel plate DBD used in this experiment is shown in figure 2.1. It consists of a Pyrex tube with an inner and outer diameter of 5.80 mm and 7.85 mm. The tube is flattened in the middle creating a 1 mm wide slit. On both sides 0.5 mm thick brass electrodes are attached measuring 37.5 by 9.3 mm. The plasma volume is therefore 0.35 cm^3. Epoxide glue is used to fix the electrodes to the glass body, which also provides a thick insulating layer to avoid breakdown of air at the edges of the powered electrode. The cable from the power source is directly soldered on one of the electrodes and the ground cable is soldered to the other electrode.
With the dimensions of the DBD known it is possible to make an estimation of its capacitance. With the dielectric constant of the Pyrex known to be 4.60 [14] the capacitance is calculated to be 2.3 pF.

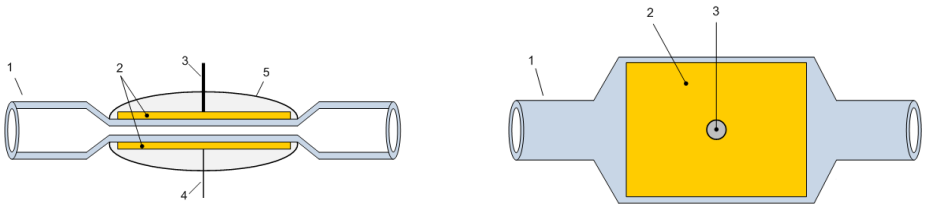

(a) Side view (b) Top view

Figure 2.1: A schematic view of the DBD. 1: Pyrex tube, 2: brass electrodes, 3: high voltage cable, 4: low voltage cable, 5: epoxide glue. The glue is not displayed in the top view.

The setup is shown in 2.2. The gas mixtures for the DBD are provided by two mass flow controllers (MFC)(Brooks 5800) with a capacity of 10 standard liters per minute (slm) and 300 standard cubic centimeter per minute (sccm) helium, respectively. Either one of the MFCs can be connected to a set of water filled bubblers which ensure that the gas flow is fully saturated. With the combination of two MFCs the humidity of the total flow can be controlled. The

setup can be fed with pure helium or a mixture of helium with 2% H_2 and 2% O_2, which is well below the explosive limit [20].

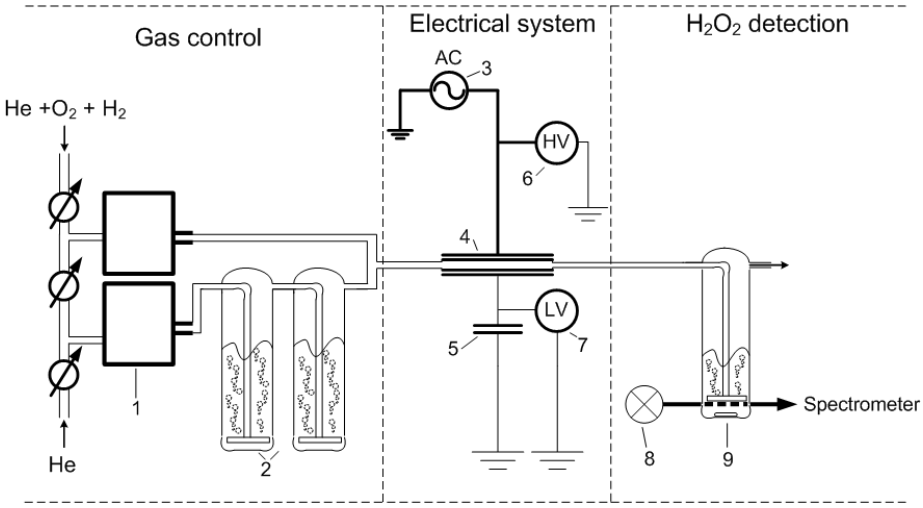

Figure 2.2: A schematic view of the setup consisting of three parts: a gas control system, an electrical system and a H_2O_2 detection system. 1: mass flow controllers (2 slm and 300 sccm), 2: bubblers filled with deionized water, 3: AC power source, 4: DBD, 5: capacitor (1nF), 6: high voltage probe, 7: 10 x voltage probe, 8: lamp, 9: bubbler containing ammonium metavanadate and a magnetic stirrer.

The DBD is powered by a high voltage AC power source (PVM500 Plasma Driver) with a range of 0 to 20 kV. A capacitor of 1 nanofarad is placed in series with the DBD which will be used to determine the charge on the plates of the DBD. The voltage over the DBD is measured by a high voltage probe (Textronix P6051A) and a 10 times voltage probe (Agilent 10x) is used to monitor the voltage over the capacitor. Both voltages are recorded by an oscilloscope (Agilent 2024A).

2.2 H_2O_2 detection

For the detection of hydrogen peroxide spectrophotometric method was used as proposed by Nogueira *et al.* [18]. The method is based on the reaction of H_2O_2 with ammonium metavanadate in an acid medium which results in the formation of an orange colored peroxovanadium cation. This chemical has maximum optical absorption at 450 nm. The Beer-Lambert law (2.1) can be used to calculate the concentration of peroxovanadium c which is directly related to the amount of reacted H_2O_2. The optical path length of the beam through the metavanadate solution d (in centimeter) is known and the molar extinction coefficient ϵ for the given wavelength is 283 mol L^{-1} cm^{-1} [18]. I_0 and I are the intensity of the transmitted light before and after H_2O_2 production, which

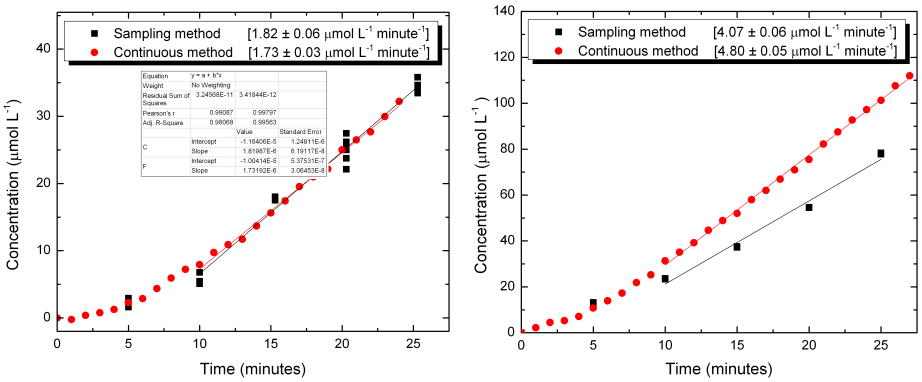

(a) 1 slm at a power of 1.17 ± 0.08 W.

(b) 2 slm at a power of 1.51 ± 0.09 W.

Figure 2.3: The results of the comparison measurements between the established (sampling) method and the continuous method. Both are measured using humid helium containing 3% water. The production rates calculated from the graphs are noted in the graphs.

will be measured. With the volume of the detection fluid known the amount of absorbed H_2O_2 can be calculated.

$$\log_{10}(\frac{I}{I_0}) = -\epsilon c d \tag{2.1}$$

To measure the H_2O_2 production the effluent of the DBD is bubbled through 40.0 ± 0.1 milliliter of ammonium metavanadate solution, which is prepared as described by [18]. An halogen lamp and a UV-VIS spectrometer (Ocean Optics HR2000) are used to determine the absorbance of the liquid at 450 nm. A proved method consists of taking a sample from the vessel, place it in a cuvette and place this in the beam path to measure the absorbance. Because the size of the cuvette is known the measurement is very accurate. However, this method has a few disadvantages: taking the sample takes time, there is a change of polluting the detection liquid and the time between the measurements has to be manually monitored. In this work the light of the lamp is coupled directly into the bubbler using an optical fiber. The light passes through the liquid under the bubbler head and is then captured by another optical fiber which is coupled to the spectrometer. This setup makes automated measurements possible and eliminates the need to interrupt the H_2O_2 production. A few measurements where made to justify this measuring method. The results are shown in figure 2.3. From the graphs it can be concluded that the new method is consistent with the established method.

The optical path length of the light beam through the vessel is measured to be 2.71 ± 0.01 centimeter. The speed of H_2O_2 production will be expressed as the rate at which the concentration in the liquid increases (which is depended of the amount of liquid used) which will be called the production rate, measured in μmol L^{-1} $minute^{-1}$.

In this work a few assumption where made: all the produced H_2O_2 is cap-

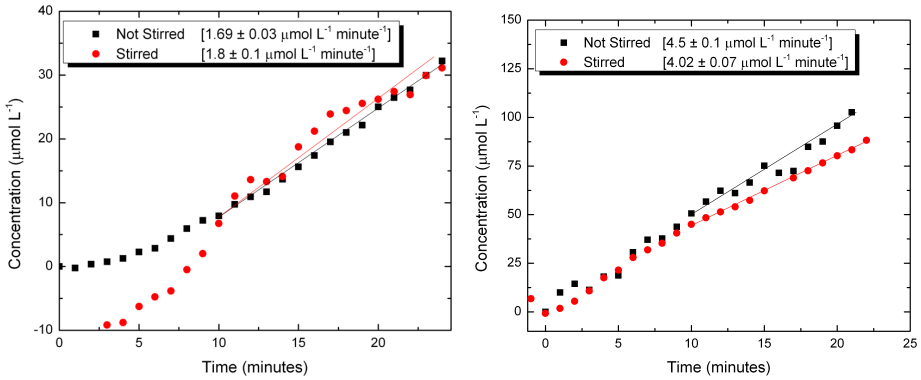

(a) 1 slm at a power of 1.16 ± 0.08 W. The non stirred production rate is 6,5% lower than the stirred rate.

(b) 2 slm at a power of 1.0 ± 0.1 W. The non stirred production rate is 12% higher than the stirred rate.

Figure 2.4: The results of the comparison measurements between stirrer and no stirrer. Both are measured using humid helium containing 3% water. The production rates calculated from the graphs are noted in the graphs.

tured in the solution and that this is equal to the amount in the discharge itself. In reality the amount in the discharge will be larger, as small parts of the H_2O_2 will dissociate immediately, attach and dissociate at the glass walls after the discharge, or pass the bubbler without being absorbed by the water. To minimize the effect of the glass walls the discharge was running for at least 10 minutes until a constant production rate is reached. The other factors can not be corrected for but needs to be kept in mind when the results of the measurements are evaluated.

2.2.1 Mixing in the metavanadate bubbler

For the H_2O_2 measurements to be accurate sufficient mixing in the metavanadate bubbler must be ensured. The bubbling of the effluent through a large part of the detection liquid can be assumed to mix most of the liquid in the detection vessel above the bubbler head. To ensure a proper mixing in the lower part of the liquid a magnetic stirrer is used. However, measuring with the stirrer requires a lot of effort because the stirrer needs to be pulled out of the way when a measurement is made with the spectrometer. For the lot of the experiments a comparison is made between measuring with and without stirrer to see how large the measuring error will be when no stirring is used. The results are shown in 2.4.

It can be concluded from these measurements that a lack of stirring introduces a slight error of about 15%. The stirrer will not be necessary in measurements where trends in production are determined. When absolute values of production are demanded the stirrer should be used.

2.3 Power measurements

Lissajous figures are used to calculate the power consumed by the DBD as firstly used by Manley [17]. For this, both the voltage over the DBD as the charge on the electrodes have to be known. The voltage is measured with the high voltage probe and the capacitor is used to determine the charge, as done by Falkenstein *et al.* [6]. Because the capacitor is placed in series with the DBD the charge on its plates matches that of the charge on the electrodes of the DBD. The capacitor has a capacitance C of 1 nF which is about 500 times that of the DBD. The capacitive voltage division ensures that the influence on the voltage across the DBD is smaller than the error in the measurement. At the same time the voltage over the capacitor will stay in the measurable region of the voltage probe. The capacitor is designed to work at high frequencies, which ensures that it acts approximately as an ideal capacitor during the measurements. The voltage over the capacitor is directly related to the charge build up on both the capacitor as the DBD. This because an (ideal) capacitor is wholly characterized by a constant capacitance, which is defined as the ratio of charge Q on each conductor to the voltage V between them: $C = Q/V$. Knowing the voltage and the capacitance the charge on the plates can be calculated.

The voltage and charge are out of phase, as can be seen in figure 2.5. A Lissajous figure is obtained when the voltage over the DBD is plotted against the charge.The surface of this figure equals the energy consumed in one AC cycle. The power can then be calculated by either dividing the energy by the duration of the cycle or by multiplying the energy with the AC frequency. In this work the energy is calculated over multiple AC cycles and therefore the first method is used to calculate the power.

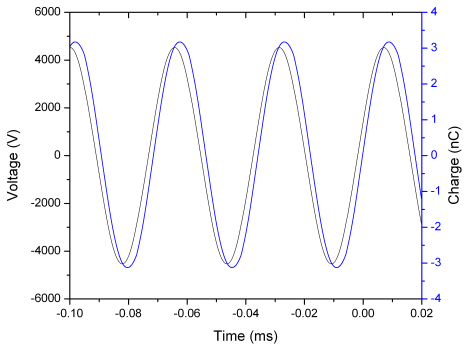

Figure 2.5: Charge and voltage plotted versus time.

An example of an ideal Lissajous figure is displayed in figure 2.6a The slopes BC and DA correspond to the discharge and AB and CD are the capacitive slopes. Figure 2.6b shows a Lissajous figure created from a measurement. The area within the Lissajous figure corresponds to the total energy consumed by one AC cycle.

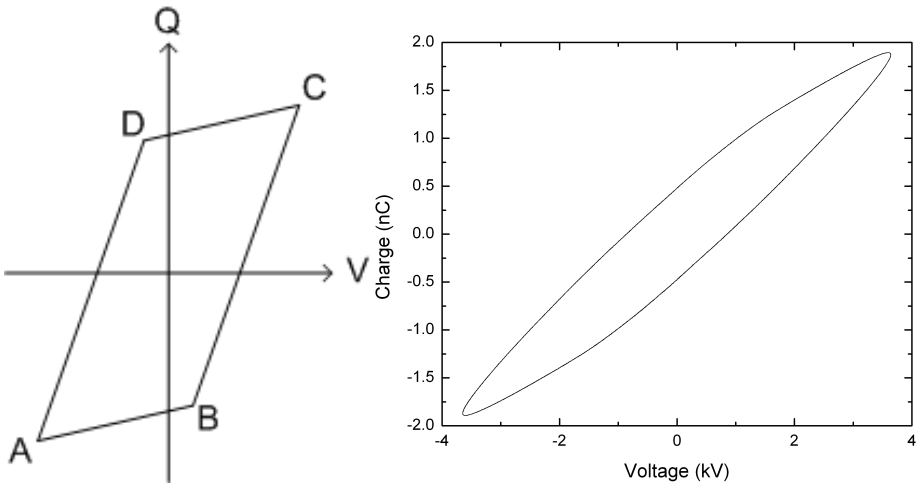

(a) An ideal Lissajous figure. (b) Lissajous figure created from a measurement.

Figure 2.6: An Ideal Lissajous figure and a figure from a measurement using helium containing 3% water.

2.4 Characteristics of the power source

The power source used has a range of 0 to 20 kV and 20 to 70 kilohertz. It has a voltage level control, a combined frequency and power switch and a duty cycle control. The power source is designed to operate at 110 volt, therefore a transformer is placed between the source and the power socket. The desired output power is obtained by a combination of the set voltage and current.
First measurements show that the output signal is strongly influenced by the set current, as shown in figure 2.7. With the current set to a high value the amplitude of the output signal is modulated with approximately 100 Hz. The difference between high and low voltage within such an envelope wave can go up to 65%. No envelope wave is observed when the current control is kept low, as can be seen in figure 2.7b. The maximum desired voltage is 10 kV which can be reached before modulation occurs.
For the rest of the experiments the current control will be as low as possible. This implies that the voltage level is set at the maximum and the current switch will be used to obtain the desired output voltage. This also implies that the frequency differs for every output voltage. Within the voltage range used in this experiment the frequency is between 20 kHz and 50 kHz. This work does not focus on the frequency settings of the source but the influence of the frequency on the functioning of the DBD should be investigated.

With the power source set to pulsed mode the output voltage is pulsed with an adjustable duty cycle. A typical voltage signal is shown in figure 2.7c. The length of the pulse plus the off-time is 5 ms and can not be changed. At the beginning of the pulse there is a peak in the voltage, which can be up to two times higher than the average pulse voltage. Because the pulse consists of over 100 AC cycles the first peak has only a limited contribution to the total power. The peak is followed by the actual voltage pulse. The oscilloscope shows that

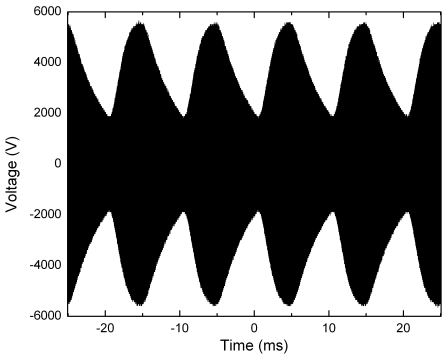

(a) Modulation of the output signal occurring when a high current is set.

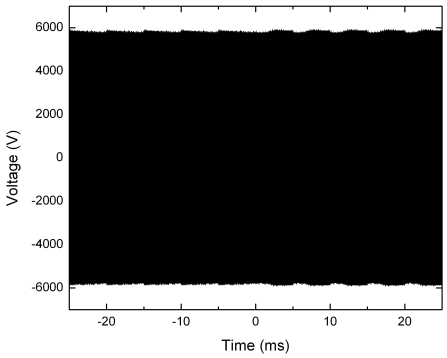

(b) No modulation when a low current is set.

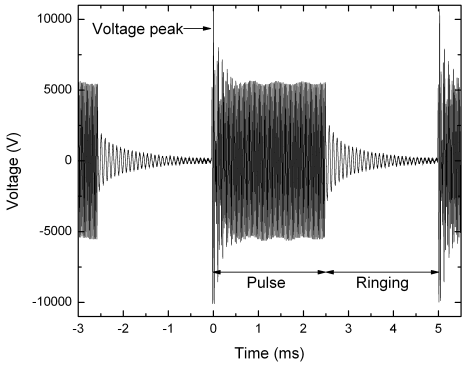

(c) The output voltage with the power source set in pulse mode. The pulse, pulse peak and ringing are indicated. The measured voltage over the capacitor shows the same behavior.

Figure 2.7: Characteristics of the used power source.

the pulses of the power source is followed by a ringing signal, which creates a tail behind every pulse. When the power is calculated this ringing is included in the integration. The power is therefore slightly higher than when only the actual voltage pulse is taken into account.

2.5 Temperature measurements

Two methods are used for the determination of the gas temperature. The first one involves fitting of the rotational band of N_2 (C-B) to obtain the rotational temperature and in the second method the rotational temperature of OH(A-X)(0-0) is obtained by making a Boltzmann plot of the resolved OH lines. To obtain measurements on both spectral lines a monochromator (Jobin Yvon) is used. Using the setup from figure 2.8 the light produced by the discharge is coupled into an optic fiber leading to the monochromator. A lens is used increase the amount of captured light. The special holder makes it possible to

capture the light from the entrance of the DBD. The N_2 method requires N_2 to be present in the discharge. When impurities in the gas are not sufficient extra N_2 should be added.

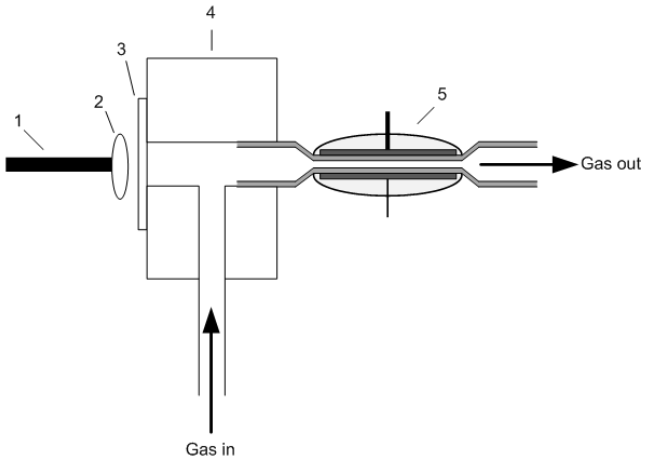

Figure 2.8: The setup used to couple the light from the discharge into the optical fiber. 1: optical fiber, 2: lens, 3: Pyrex plate, 4: PVC holder, 5: DBD.

For the rotational temperature of N_2 the rotational band at 337 nm is measured. The shape of this band, especially its tail, is influenced by the rotational temperature. If the gas temperatures in the DBD differ for various settings this should be seen in the nitrogen line. Specair [7] is used to simulate nitrogen lines at various temperatures. Comparing these to the measured lines the temperature of the gas can be determined. An example of a used N_2 peak is shown in figure 2.9a.

The OH lines around 310 nm are used to determine the temperature using a Boltzmann plot. For the intensity of the lines a Boltzmann distribution is assumed. The intensity of a peak caused by the transition from state n to m is then given by:

$$I_{nm} = N_n A_{nm} h\nu_n m \tag{2.2}$$

Where N_n is the number of molecules in the initial state, A_{nm} is a molecular constant for the transition probability and $h\nu$ is the energy of the emitted photon. For an equilibrium state N_n is given by:

$$N_n = N_0 \exp\Big(\frac{-E_n}{k_B T}\Big) \tag{2.3}$$

With N_0 a contant, E_n the energy of state n, T the temperature and k_B the Boltzmann constant. E_n is dependent on the rotational constant B_R and the rotational quantum number J as:

$$E_n = B_R J(J+1) \tag{2.4}$$

When n is a degenerate state the total number of molecules in the state is used which can be calculated J:

$$N_n^* = N_n(2J+1) \tag{2.5}$$

Using $\nu_{nm} = c/\lambda_{nm}$ this can be written as:

$$\ln\Big(\frac{I_{nm}\lambda_{nm}}{A_{nm}(2J+1)}\Big) = ln(N_0hc) - \frac{E_n}{k_BT} \tag{2.6}$$

A_{nm} and E_n are known [3] [4]. Plotting the left side of the equation versus the energy of the state results in a line with a slope equal to $-1/k_BT$. From here the temperature is easily calculated.This method is valid for low rotational numbers [2]. The calculated temperature can approximately be taken as the gas temperature [21]. An example of a Boltzmann plot is shown in figure 2.9b. The slope of the fit is -0.00292 cm, which corresponds to a temperature of 492 K.

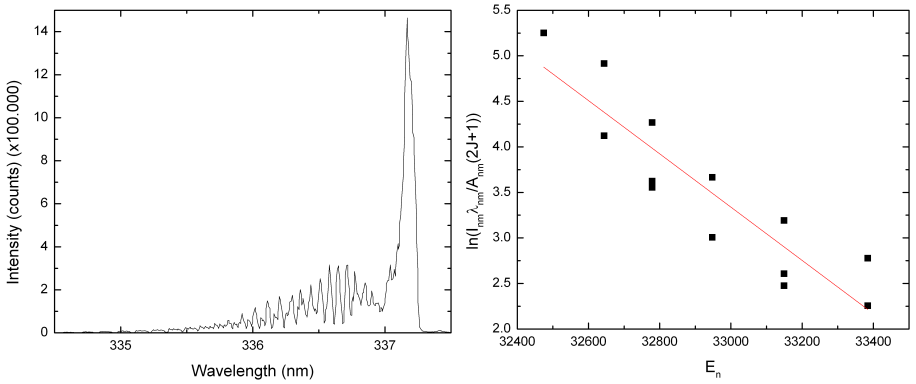

(a) An example of a N_2 (C-B) rotational band. (b) An example of a Boltzmann plot. The slope of the fit is -0.00292 cm.

Figure 2.9: Techniques used for temperature measurements

2.6 Measurements

First measurements are done using 1 and 2 slm humid helium. A maximum water content will be used, which will be around 3%. The power will be varied within the available range, using step sizes of 1 watt. From these measurements the power with optimal efficiency will be deduced which will be used in later experiments.
Next the effect of a pulsed voltage will be investigated. The power source will be set to deliver a pulse with a duty cycle of 50%. The power will be variated as with the first measurement.
During the final measurement on humid helium the water concentration will be varied. The power will be fixed at the optimum value found in the first measurement.

For the H_2-O_2 mixture a 1 slm measurement will be done with varying power as with the first measurement on helium.
During the project time no full measurements series can be done on the flow rate and the pulsed power mode. However a few measurements will be done to

see if the behavior using the mixture matches that of the humid helium. For the flow rate two measurements will be done at different powers. These consist of one measurement at 2 slm and a control measurement at 1 slm. For the pulsed power mode again a control measurement was done, followed by a 15 and 50% duty cycle measurement at the same voltage as the control. Finally an extra 50% duty cycle measurement will be done at a different voltage.

After this temperature measurements will be made. The power and flow rate settings where reproduced for the measurement of the nitrogen and OH lines. For completeness overview spectra will be made, using the Ocean Optics spectrometer.

Chapter 3

Results and discussion

When the reactor is turned on it emits a purple to pink light, which turns to blueish white when water vapor is added or when the H_2-O_2 mixture is used. The brightness increases on higher powers. At least 1.3 kilovolt is needed to establish a stable discharge. Current-voltage measurements show that the discharge is diffuse.

3.1 Results using humid helium

First the performance of humid helium was investigated. A typical result is shown in figure 3.1, which shows the production rate and efficiency for various input powers for a 2 slm flow containing 3% water. A rising production is shown for increasing power but the efficiency seems to have a maximum around 1 W. At higher powers the efficiency seems to saturate.

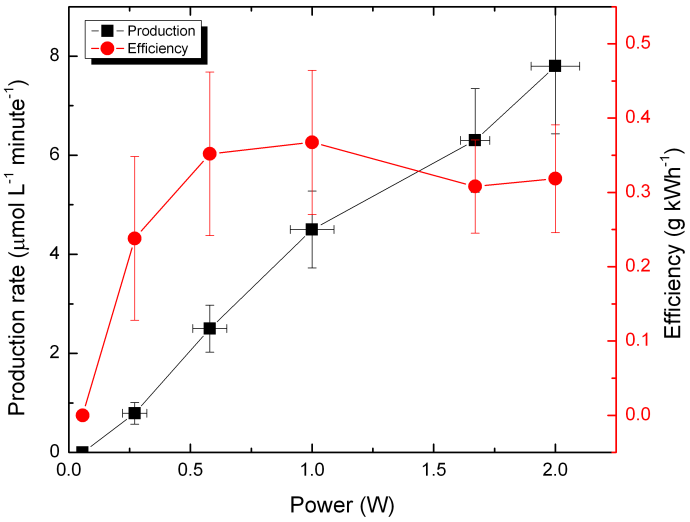

Figure 3.1: The production rate plotted versus power. The DBD was operating with a 2 slm helium flow containing 3% water. The power source was in continuous mode.

In figure 3.2 the results from the other measurements on humid helium are summarized. Along with the 2 slm measurement the results of the 1 slm measurement are plotted. Also a 2 slm measurement with a 50% duty cycle is displayed in the graphs.

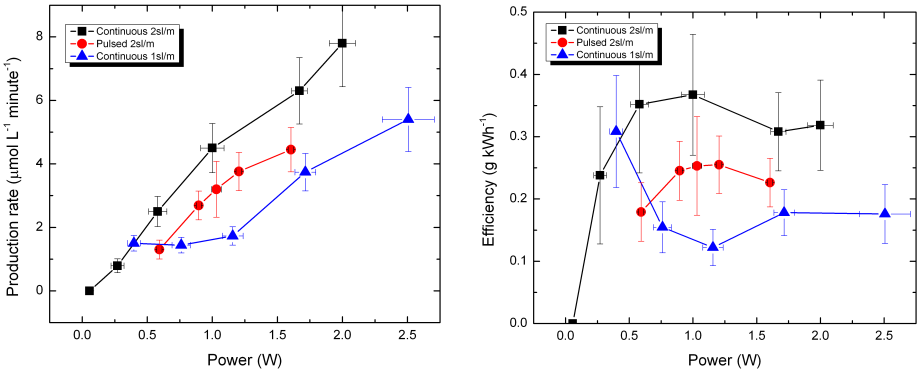

(a) Production (b) Efficiency

Figure 3.2: The production rates and efficiencies at different power settings plotted versus power. In all cases humid helium was used, containing 3% water. In case of the pulsed power source mode the time averaged power is used.

The behavior of the DBD changes with different flow rates. In case of the 2 slm flow the production increases as described above. At 1 slm the production starts of at a similar value as in the 2 slm case, but the production does not increase between approximately 0.25 and 1.25 W. After this the production increases linearly with power. For both flows the efficiency saturates when the power increases above about 1.7 W.

What causes the difference in behavior for the 1 and 2 slm cases is not yet understood. Many parameters change when the flow rate is increased.; not only the availability of molecules increases but also the gas temperature changes, since more flow implies more cooling. Also the flow speed increases. An increasing flow speed results in a decrease in residence time; the time the molecules are in the plasma. If the availability of molecules was a key factor in this behavior, then the yield and product efficiency would scale with changes in the flow. This is not the case as can be seen from the figure. The temperature could have a leading role, since the difference in production rate increases with power. The temperature for the 1 slm case could be too high to produce H_2O_2 efficiently as H_2O_2 dissociates easily at higher temperatures. When assumed that there is more cooling in the 2 slm case, the temperatures should remain lower. This explanation does not account for the saturation after 1.7 W, because higher powers should results in more heat generation, thus a higher temperature and therefore a lower efficiency. Temperature measurements should give a better insight into this.

Furthermore it should be investigated if the efficiency keeps rising in the 1 slm case for powers lower than used in this experiment as the results indicate.

To obtain trustworthy values of the production measurements where done

using a magnetic stirrer to ensure sufficient mixing in the measuring vessel. Production rates and efficiencies where obtained for a 1 W input power using 1 and 2 slm helium containing 3% water. The result show to be in line with the measurements without stirring.

Flow rate (slm)	Power (W)	Production rate (μmol L^{-1} $minute^{-1}$)	Efficiency (g kWh^{-1})
1	0.9 ± 0.1	1.94 ± 0.04	0.17 ± 0.02
2	1.0 ± 0.1	3.65 ± 0.04	0.31 ± 0.04

Table 3.1: Results of measurement using a magnetic stirrer. Humid helium was used, containing 3% water.

3.1.1 Pulsed mode

When the results form the pulsed and continuous power source mode are compared it is notable that the overall behavior is the same: the efficiency in the pulsed mode also has a peak around 1 W. The production and efficiency are lower in the pulsed mode which was not expected. What is striking though is that the production and efficiency are lower in pulsed mode than in continuous mode while it was expected to be the other way around. As stated in section 1.2, the pulsed mode was supposed to give a lower average gas temperature and a higher electron temperature and thereby a lower dissociation rate for the H_2O_2 and a larger amount of radicals. The efficiency was therefore expected to increase, but the results show that this is not the case.

The lower production could be caused by the high flow rate. The air gap of the DBD is known to be 1 mm high, 10 mm wide and 37.5 mm long. Therefore a flow of 2 slm results in a velocity of the particles through the discharge of 3.3 m/s. The residence time is then calculated to be 11 ms The pulse length is 2.5 ms which means that the particles are threated for a maximum of 6 ms. The decreasing productivity could mean that there is a minimum treatment time needed for an efficient production.

3.1.2 Varying water contents

Figure 3.3 shows the production under various humidities of the helium. The combination of the available flow controllers limits the range of humidity levels that can be achieved: there is a humidity region from 0,68% to 2,25% that can not be reached. Outside this region multiple measurements where done.
The graphs show a linear increase of production with the humidity. Because the power is not varied the efficiency is proportional to the production and therefore shows the same linear behavior. Apparently the efficiency at a fixed power setting and flow is proportional to the available water molecules in the flow.

3.2 Results on H_2-O_2 mixture

The results of the measurements using the H_2-O_2 mixture are shown in figure 3.4 along with results of comparable measurements on humid helium.

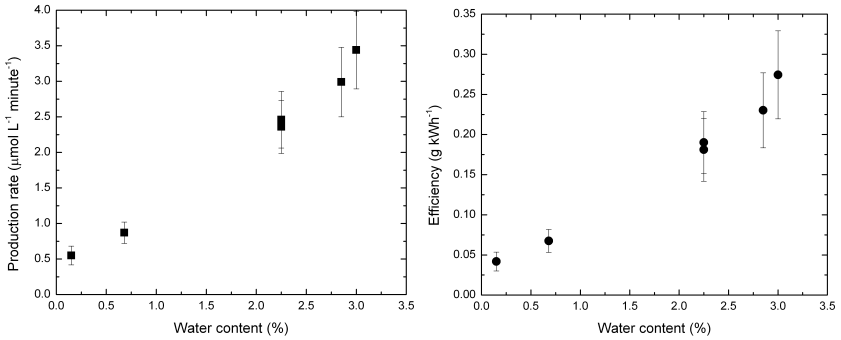

(a) Production (b) Efficiency

Figure 3.3: The production rates and efficiencies plotted versus the water content. The flow was set to 2 slm and the power was measured to be 1.06 ± 0.06 W.

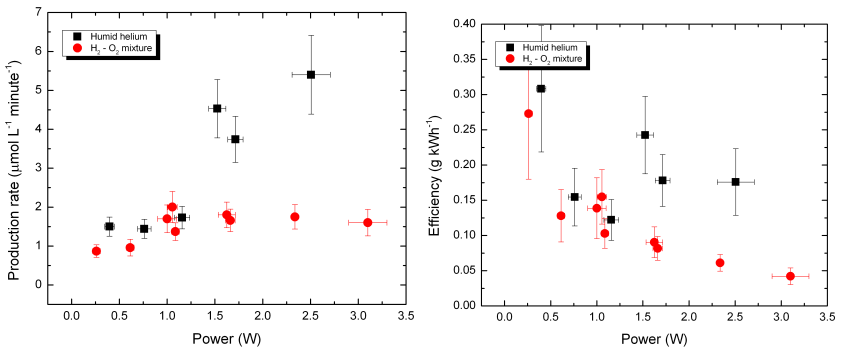

(a) Production (b) Efficiency

Figure 3.4: The production rates and efficiencies using 1 slm humid helium(3% water) and 1 slm H_2-O_2 mixture.

As can be seen, the production using the mixture does not depend as strongly on the applied power as in it is in the case of the humid helium. At first the production rises and resembles that of the humid helium. Around 1 W it becomes constant, while in the humid helium discharge case the production continuous to increase with increasing power. Where the humid helium shows a rise in production the production of the mixture stays at the same level. The second graph shows that the efficiency decreases for higher powers and the graph resembles an exponential decay. Apparently a stoichiometric gas mixture is not the key to higher efficiencies.

The behavior of the DBD differs greatly when either the humid helium or the gas mixture is used. The efficiency using the mixture is lower than when using the humid helium which is contrary to expectations stated in section 1.2. The same can be said about the decay in production for higher powers: it saturates at 1 W instead and does not increase with power as expected

With the goal of further investigating if the characteristics using H_2-O_2 mixture differ from the humid helium measurements where made comparing flow rates of 1 slm and 2 slm. Further the influence of pulsed power source modes are investigated. The results are shown in figures 3.5 and 3.6.

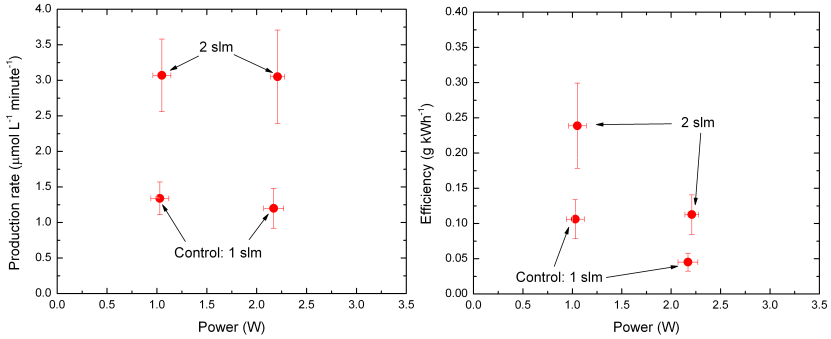

(a) Production rate. (b) Efficiency

Figure 3.5: Characteristics using the H_2-O_2 mixture regarding the flow rate. Measurements where done to compare a 2 slm flow rate to the 1 slm flow rate.

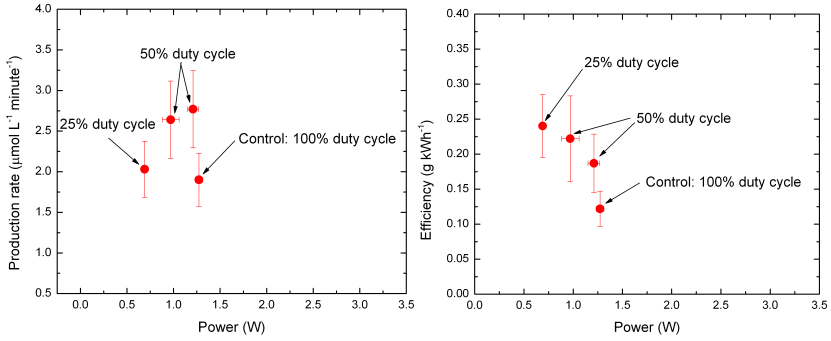

(a) Production rate (b) Efficiency

Figure 3.6: Characteristics using the H_2-O_2 mixture regarding power source mode. Pulsed measurements where done at approximately 4 kilovolt using 1 slm. A shorter pulse length therefore yields a lower overall power.

zijn

From figures 3.5 it can be seen that the production rate and efficiency increases with flow rate as was seen earlier with the humid helium. Because a small number of measurement where taken there is no information about saturating behavior, like seen with the humid helium.

3.2.1 Pulsed mode

Figure 3.6 shows that in the case of the H_2-O_2 mixture the efficiency increases when the pulsed power is used. This in contrary to the case of humid helium,

where the production and efficiency seemed to be lower in the pulsed mode.

However, two properties of the discharge differ in the pulsed mode: the flow rate and the gas mixture.

For the humid helium a flow rate of 2 slm was used while for the H_2-O_2 mixture is was only 1 slm. Therefore the speed of the particles through the DBD is lower in the mixture case, and thus the residence time is higher. For the 2 slm case it was 11 ms, so for the 1 slm case it is 22 ms. The treatment time is also doubled, what could be enough for a more efficient production. Additional measurements using a 1 slm flow of humid helium could give more insight in this issue.

The influence of the change in gas mixture could be in the the reaction rates of the reactions involving H_2 and O_2. As can be seen from figure 1.1b in section 1.2 the H- and O-radical production increases with electron temperature. Assumed is that the electron temperature is higher in the pulsed mode because of the higher applied voltage. Therefore the availability of reactive particles increases and the production of H_2O_2 could be stimulated.

3.3 Overview spectra and temperature measurements

Overview spectra where made using either humid helium or the H_2-O_2 mixture. The results are shown in figure 3.7. The He and H lines show up, just like the OH(A-X) band and the H_2-Fulcher α-band in the case of the H_2-O_2 mixture. Using the mixture results in a continuum signal, caused by the hydrogen in the mixture.

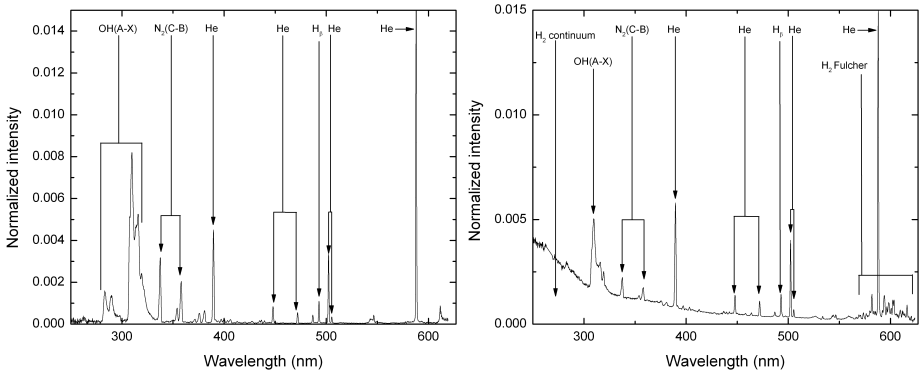

(a) Humid helium. (b) H_2-O_2 mixture

Figure 3.7: A spectral overviews for the DBD operating at 1 W and 2 slm. The species associated with the peaks are indicated.

The temperature of the discharge plasma is measured in two ways: by fitting the N_2(C-B) band to obtain the rotary temperature of N_2 and by obtaining a Boltzmann plot to determine the rotational temperature of OH(A-X). The overview spectra show that nitrogen is present in the discharge. However, for

Reaction	Reaction rate	
	300 K	400 K
OH + OH + M→ H_2O_2+ M	1.33×10^{-11}	0.98×10^{-11}
$H_2O_2 \rightarrow$ 2 OH	1.24×10^{-40}	2.8×10^{-32}
H + $H_2O_2 \rightarrow H_2O$ + OH	5.1×10^{-14}	2.7×10^{-13}

Table 3.2: H_2O_2 producing and destructing reactions with their reaction rates at 300 and 400 K

the high resolution spectra it is not sufficient. Therefore 5 sccm of nitrogen was added to the gas mixture to perform these measurements.

The results of the nitrogen measurements are shown in figure 3.8 and figure 3.9. Various settings of the DBD all resulted in indistinguishable nitrogen spectra. Therefore no distinction in temperature was found for the various settings. The temperature of the profiles match that of a simulated profile of 350 ± 50 K.

For three different water contents the temperature was determined using a Boltzmann peak fitting on the OH spectral lines. The result is shown in 3.10. The calculated temperatures are about 460 K, with an error of 150 K. The large error shows the inaccuracy of this measurement.

From the results no difference on the temperature can be seen when using different settings on the DBD. Because of the large errors they can not be used to relate the temperature of the gas in the DBD to the production and efficiency. If the gas temperature plays a role in the production and efficiency, it should be due to fluctuations of the order of 50 K. In table 3.2 it can be seen that even within this range the reaction rates for the H_2O_2 producing and destroying rates change significantly. Therefore more accurate temperature measurements should be done in future researches.

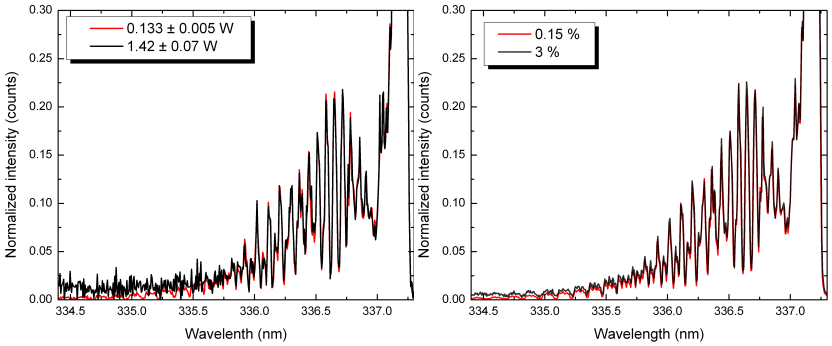

(a) Variated power. (b) Variated water content.

Figure 3.8: A part of the tail of the N_2 peak for various settings. All intensities are normalized. For the power variated measurements 3% water was used. The power on the variated water content measurements was 0.76 ± 0.03 W. The shape of tail tale does not change when the settings are varied.

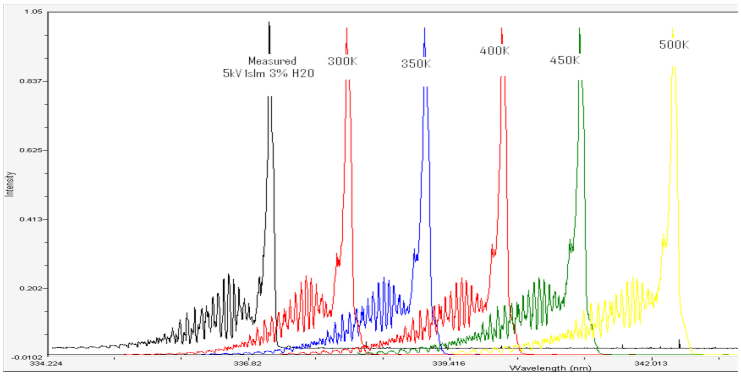

Figure 3.9: A measured N_2(B-C) band plotted with simulated bands.

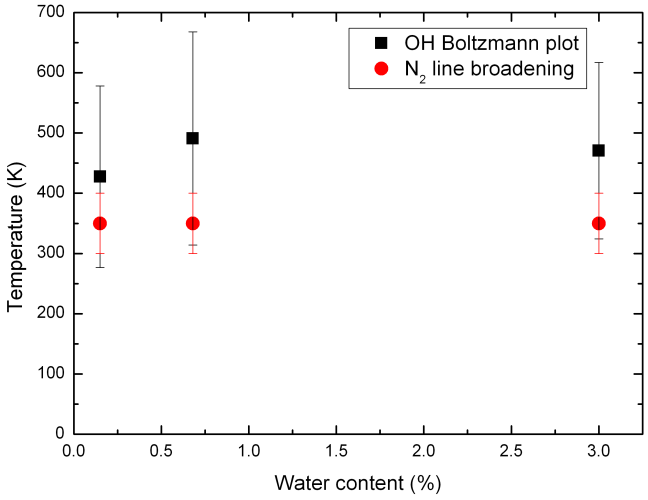

Figure 3.10: Measured temperatures at different water contents, obtained by analyzing OH(A-X) and N_2(B-C) bands. In the H_2-O_2 mixture also the temperature of 350 ± 50 K was found using the N_2(B-C) rotational temperature.

Chapter 4

Conclusion

The characteristics of the hydrogen peroxide production using a DBD setup are investigated using humid helium and a mixture of helium, hydrogen and oxygen. The results are summarized.

The measurements on humid helium show that the production rate and efficiency of the H_2O_2 production process is influenced by various parameters. In all cases increasing powers yield more production. However, the behavior of the efficiency under different powers is strongly depended on the flow rate used. Production and the water content of the helium seem to be linear related. Using a pulsed voltage signal resulted in lower efficiencies, which is against expectations. This indicates that there exists a minimum residence time for efficient production. Highest efficiencies for current experimental conditions are reached using 2 slm helium containing 3% water at 1.0 ± 0.1 watt: 0.31 ± 0.04 g kWh^{-1}. This of the same order of magnitude as the production reached by Kirkpatrick in an argon DBD [12].

The measurements on the hydrogen and oxygen mixture show that increasing powers do not yield more production for this gas mixture. The efficiencies therefore go down with power. Using a pulsed power source improved the production, as using a higher flow.

The results show that the behavior of the DBD is strongly influenced by the used gas mixture. In the lower power region the behavior of the H_2-O_2 mixture is similar to humid helium but above 1 watt the production and efficiencies are lower. The flow rate is also of large influence, which is especially shown in this report for the humid helium.

For the H_2-O_2 mixture it is seen that the production increases when a pulsed power is used, in which the behavior differs from the humid helium. This is probably caused by a combination of the lower flow rate and a larger electron temperature dependency of the radical creating reactions.

The temperature is suspected to influence the processes in the DBD, but no distinction could be made with the temperature measurements done. The rotational temperature of the N_2(C-B) was estimated to be 350 ± 50 K while the rotational temperature of the OH(A-X) lines showed a temperature of 460

Author	Efficiency (g kWh^{-1})	Gas mixture	Power (W)	Power density (W/cm^3)	Residence time (s)
Current results	0.31	Humid He (3% H_2O)	1.0	2.86	11×10^{-3}
Current results	0.24	H_2(2%)+O_2(2%) +He	0.69	1.86	22×10^{-3}
Kirkpatrick *et al.* [12]	0.14	Humid Ar (3% H_2O)	1.33	8.47	4.7×10^{-3}
Zhao *et al.* [22]	80.8	H_2(95.2)+ O_2(4.8%)	3.5	0.23	18

Table 4.1: Efficiencies from multiple experiments.

± 150 K. More accurate temperature measurements are necessary to establish the effect of gas temperature of the production of H_2O_2.

In table 4.1 the results from this project are compared with results from literature. As can be seen the efficiencies reached are in line with the results of Kirkpatrick *et al.* who used a simular DBD. The results from this work are about twice as high. Kirkpatrick used a much higher power density, but also a lower residence time. Therefore it seems that the influence of the residence time is again emphasized. This is even more the case when looking at the work of Zhao *et al.* He reached efficiencies which are more than 200 times higher but with a lower power density. The residence time of 18 s is probably the reason for the high efficiency. Future research should therefore look more into the influence of residence time on the efficiency of the H_2O_2 production process.

Bibliography

[1] NIST Chemical Kinetics Database, Standard Reference Database 17.

[2] Peter Bruggeman and Daan C Schram. On OH production in water containing atmospheric pressure plasmas. *Plasma Sources Science and Technology*, 19(4):045025, August 2010.

[3] I.L. Chidsey and D.R. Crosley. Calculated rotational transistion probabilities for the A-X system of OH. 13, 1979.

[4] G H Dieke and H.M. Crosswhite. The ultraviolet bands of OH. 2(87):97–199, 1961.

[5] B Dodet, E Odic, A Goldman, M Goldman, and D Renard. Hydrogen Peroxide Formation by Discharges in Argon/Water Vapor Mixtures at Atmospheric Pressure. *Journal of Advanced Oxidation Technologies*, 8(1):91–97, 2005.

[6] Zoran Falkenstein and John J Coogan. Microdischarge behaviour in the silent discharge of nitrogen - oxygen and water - air mixtures. *Journal of Physics D: Applied Physics*, 30(5):817–825, March 1997.

[7] D. Fletcher, J.-M. Charbonnier, G.S.R. Sarma, and T. Magin. Radiation and Nonequilibrium Collisional-Radiative Models, 2002.

[8] G.J.M. Hagelaar and L.C. Pitchford. Bolsig+-software based on "Solving the Boltzmann equation to obtain electron transport coefficients and rate coefficients for fluid models". *Plasma Sources Sci. Technol.*, 14:722–733, 2005.

[9] Dan Hâncu, Jordan Green, and Eric J Beckman. H(2)O(2) in CO(2): sustainable production and green reactions. *Accounts of chemical research*, 35(9):757–64, September 2002.

[10] John T Herron and David S Green. Chemical Kinetics Database and Predictive Schemes for Nonthermal Humid Air Plasma Chemistry . Part II . Neutral Species Reactions 1. *Reactions*, 21(3), 2001.

[11] Zhao Jianli, Zhou Juncheng, Su Ji, Guo Hongchen, Wang Xiangsheng, and Gong Weimin. Scale-Up Synthesis of Hydrogen Peroxide from H 2 /O 2 with Multiple Parallel DBD Tubes. *Plasma Science and Technology*, 11(2):181–186, April 2009.

[12] M J Kirkpatrick, B Dodet, and E Odic. Atmospheric Pressure Humid Argon DBD Plasma for the Application of Sterilization - Measurement and Simulation of Hydrogen , Oxygen , and Hydrogen Peroxide Formation. *International Journal of Plasma Environmental Science & Technology*, 1(1):96–101, 2007.

[13] Ulrich Kogelschatz. Dielectric-barrier Discharges : Their History , Discharge Physics , and Industrial Applications. 23(1):1–46, 2003.

[14] David R Lide and Grace Baysinger. CRC Handbook of Chemistry and Physics 92nd Edition Internet Version 2012. pages 2012–2012, 2012.

[15] D X Liu, P Bruggeman, F Iza, M Z Rong, and M G Kong. Global model of low-temperature atmospheric-pressure He + H 2 O plasmas. *Plasma Sources Science and Technology*, 19(2):025018, April 2010.

[16] Bruce R Locke and Kai-Yuan Shih. Review of the methods to form hydrogen peroxide in electrical discharge plasma with liquid water. *Plasma Sources Science and Technology*, 20(3):034006, June 2011.

[17] T. C. Manley. The electric characteristics of the ozonator discharge. *October*, 16(1909):450–460, 1943.

[18] Raquel F Pupo Nogueira, Mirela C Oliveira, and Willian C Paterlini. Simple and fast spectrophotometric determination of H(2)O(2) in photo-Fenton reactions using metavanadate. *Talanta*, 66(1):86–91, March 2005.

[19] I A Soloshenko, V V Tsiolko1, S S Pogulay1, A G Terent'yeva1, V Yu Bazhenov1, A I Shchedrin1, A V Ryabtsev1, and A I Kuzmichev2. The component content of active particles in a plasma-chemical reactor based on volume barrier discharge. *Plasma Sources Sci. Technol*, 16(56), 2007.

[20] V Schroeder and K Holtappels. Explosion Characteristics of Hydrogen-Air and Hydrogen-Oxygen Mixtures at Elevated Pressures. *Iinternational conference on hydrogen safety*, 2005.

[21] T Verreycken, D C Schram, C Leys, and P Bruggeman. Spectroscopic study of an atmospheric pressure dc glow discharge with a water electrode in atomic and molecular gases. *Plasma Sources Science and Technology*, 19(4):045004, August 2010.

[22] Jianli Zhao, Juncheng Zhou, Ji Su, Hongchen Guo, Xiangsheng Wang, and Weimin Gong. Propene Epoxidation with In-Site H 2 O 2 Produced by H2/O2 Non-Equilibrium Plasma. *AIChE Journal*, 53(12):2–7, 2007.

[23] Juncheng Zhou, Hongchen Guo, Xiangsheng Wang, Mingxing Guo, Jiangli Zhao, Lixing Chen, and Weimin Gong. Direct and continuous synthesis of concentrated hydrogen peroxide by the gaseous reaction of H2/O2 non-equilibrium plasma. *Chemical communications (Cambridge, England)*, (12):1631–3, March 2005.